



HAL
open science

Vapothermal curing of hemp shives: Influence on some chemical and physical properties

Reine Karam, Nor-Edine Abriak, Hicham Khouja, Frederic Becquart

► **To cite this version:**

Reine Karam, Nor-Edine Abriak, Hicham Khouja, Frederic Becquart. Vapothermal curing of hemp shives: Influence on some chemical and physical properties. *Industrial Crops and Products*, 2021, 171, pp.113870. 10.1016/j.indcrop.2021.113870 . hal-03772263

HAL Id: hal-03772263

<https://hal.science/hal-03772263v1>

Submitted on 22 Aug 2023

HAL is a multi-disciplinary open access archive for the deposit and dissemination of scientific research documents, whether they are published or not. The documents may come from teaching and research institutions in France or abroad, or from public or private research centers.

L'archive ouverte pluridisciplinaire **HAL**, est destinée au dépôt et à la diffusion de documents scientifiques de niveau recherche, publiés ou non, émanant des établissements d'enseignement et de recherche français ou étrangers, des laboratoires publics ou privés.



Distributed under a Creative Commons Attribution - NonCommercial 4.0 International License

1 Vapothermal curing of hemp shives: influence on some chemical and physical properties

2

3 Reine Karam ^{a,b}, Frederic Becquart ^{a,b,*}, Nor-Edine Abriak ^{a,b}, Hicham Khouja ^a

4

5 ^a *IMT Lille Douai, Institut Mines-Télécom, Centre for Materials and Processes, F-59000 Lille, France*

6 ^b *Univ. Lille, Institut Mines-Télécom, Univ. Artois, Junia, ULR 4515 - LGCgE – Laboratoire de Génie
7 Civil et géoEnvironnement, F-59000 Lille, France*

8

9 Abstract

10 In a perspective of a sustainable development, a new generation of construction materials based on
11 renewable plant resources has emerged to face environmental issues. However, the formulation of
12 structural vegetal concretes (based on plant aggregates, a mineral binder and water) requires to
13 enhance the compatibility of plant aggregates and binder.

14 This paper presents an experimental study that evaluates the influence of vapothermal treatment, a
15 promising method of cure under saturated water vapour pressure, on chemical composition and
16 physical properties (loss of mass, absorption, and specific gravity) of hemp shives, entering in the
17 composition of vegetal concrete. Indeed, developing bio-based concrete by vapothermal curing
18 requires identifying the appropriate curing conditions both from the point of view of the hemp
19 aggregates and the binder. In particular, these curing conditions must respect a compromise between
20 the preservation of the physical and chemical properties of hemp shives and an efficient curing of the
21 binder.

22 Several levels of curing temperatures were defined between 150 and 230°C (carbonization) and results
23 of Treated Hemp Shives (THS) were compared with those of Raw Hemp Shives (RHS). The
24 experimental results showed physical modifications explained by chemical transformations that affects
25 the hemicellulose, cellulose and lignin composition of TSH and modifies the structure of hemp shives.
26 The effect of vapothermal curing on hemp shives was determined through X-Ray Diffraction XRD
27 and thermogravimetry TG. The loss of mass of THS increases as the curing temperature increases and
28 specific gravity decreases. As for water absorption, which relates to the hydrophilic character of the
29 treated hemp shives, it decreases slightly. This experimental study made it possible to assess the
30 interest of a vapothermal curing in a prospect of using hemp shives in binder interaction in order to
31 perform structural vegetal concrete.

32

33 Keywords: *Vapothermal treatment; Hemp shives; Chemical transformations; Binder interaction*

34

35 1. Introduction

36 The building sector is known to be responsible for one of the world's main sources of CO₂ emissions,
37 through the production of building materials and the energy consumption of buildings in the operating

38 phase: heating, ventilation and air conditioning (United Nations Environment Programme, 2009). In
39 France, this sector represents 44% of the energy consumed, i.e. more than 120 million tons of CO₂
40 each year (Commissariat Général au Développement Durable, 2020). Particularly, the cement industry
41 is responsible of large volumes of CO₂ emitted during the manufacture of Portland cement clinker
42 (Gartner, 2004). Today, most research efforts are focused on the production of building materials that
43 help reduce environmental impact and can promote sustainable development and circular economy.

44
45 Among the materials developed that can meet these challenges, vegetal concretes are promising. They
46 are composed by the association of vegetal aggregates with a mineral binder. Binders based on cement
47 or lime are mainly used (Amziane and Arnaud, 2013). The positive environmental impact of these
48 materials in terms of their contribution to the fight against global warming is due to the biogenic
49 carbon stored by plant aggregates. It corresponds to the atmospheric CO₂ absorbed during the
50 photosynthesis of plants and trapped inside the material during its entire life cycle, thus reducing its
51 carbon footprint (Amziane, 2016). Vegetal concretes are rather oriented towards non-structural
52 applications as insulation, coatings, noise barriers, etc. Research works are multiplied to try to develop
53 structural vegetal concrete. However, in this case, cement remains the binder that guarantees good
54 mechanical performance.

55
56 Nevertheless, the deployment of vegetal concretes in construction applications is limited by various
57 problems encountered after introducing plant aggregates in the binder. The hydrophilic nature of plant
58 aggregates can lead to a decrease in the amount of water available for hydration of the binder (Jami et
59 al., 2019; Nozahic, 2012). Water absorption by these lignocellulosic aggregates leads to water
60 additions to the mix to preserve the workability of the concrete, resulting in low mechanical strengths.
61 These quantities of water can solubilize some extractible molecules from plant aggregates, such as
62 polysaccharides (sugars), pectins, tannins, or waxes. Some of these molecules are capable of reacting
63 with the binder, modifying the hardening of the materials (Amziane and Arnaud, 2013). The fraction
64 of water not consumed by binder hydration must then be removed. It follows that one of the major
65 problems reported for lignocellulosic concretes is drying, especially as the material is more heavily
66 loaded with lignocellulosic materials. In addition, experience shows dimensional instability of vegetal
67 concretes (Hillis, 1984). This phenomenon is to be correlated with the important water recovery of the
68 vegetable aggregates and thus of the vegetal concretes. So, a lot of researches were carried out to
69 improve the compatibility between the plant aggregates and the binder (Aderinsola Sadiku and Sanusi,
70 2014; Khazma et al., 2014, 2012, 2011; Miranda de Lima et al., 2015; Pasca et al., 2010).

71
72 Among the different approaches used generally for energy recovery from biomass, can be found the
73 hydrothermal treatment (Funke et al., 2013; Huang and Yuan, 2016; Rulkens, 2008; Shafie et al.,
74 2018). It is a process in which, biomass is heated and converted into useful resources in water or other

75 suitable solvents at certain temperatures and pressures (Krylova and Zaitchenko, 2018; Toor et al.,
76 2011; Vogel, 2019). Many studies have investigated hydrothermal treatment and its influence on
77 biomass (Krylova and Zaitchenko, 2018; Olszewski et al., 2020; Peterson et al., 2008; Sevilla and
78 Fuertes, 2009; Sharma et al., 2020; Titirici et al., 2015; Volpe et al., 2020). When the treatment occurs
79 in saturated vapor instead of being submerged in water, it is called vapo-thermal treatment. This curing
80 on biomass has been patented in 2009 (German Patent Nr. DE 10 2009 010 233 A1, 2009), **but there is**
81 **a lack of published studies on vapo-thermal treatment (Funke et al., 2013; Shafie et al., 2018; Yeoh et**
82 **al., 2018)**. Researchers have reported that the treatment in or outside water can have an effect on the
83 carbon composition of treated vegetals (Funke et al., 2013). As the vapo-thermal treatment can be
84 considered as a hydrothermal treatment where the water is in its gaseous form, there is often confusion
85 between the two terms. In 1913, it was suggested by Bergius that hydrothermal reactions were
86 responsible for the formation of fossil fuels, particularly coal. At low temperatures between 180 and
87 250°C, this treatment is known as carbonization. The main product is a hydrochar which has a similar
88 property to that of a low-rank coal. At intermediate temperature ranges between 250 and 375°C, the
89 process is known as liquefaction, resulting in the production of a liquid fuel (biocrude) that can be
90 upgraded to petroleum-derived products. At higher temperatures above 375°C, the process is known as
91 gasification, resulting in the production of a syngas (Biller and Ross, 2016; Huang and Yuan, 2016). It
92 is interesting to note that most of the papers focus on rather severe reaction conditions, mainly above
93 250°C (Guillot, 2019).

94

95 At the same time, vapo-thermal treatments have been used in construction materials domain and have
96 led to a significant influence on the mechanical properties of the Ultra High Performance Concrete
97 (Galvankova et al., 2016). Through autoclaving, the degree of hydration of these **sand-lime**
98 **(autoclaved aerated concrete (AAC) and dense bricks)** have been considerably increased. The main
99 reasons for the improved mechanical properties are the formation of a homogeneous cement paste
100 matrix, consisting of closely connected Calcium Silicate Hydrates C-S-H crystalline fibers, which
101 develop a more stable structure than amorphous C-S-H phases formed in Ordinary Portland Cement
102 OPC (Fontana et al., 2009). Vapo-thermal treatment has also shown positive effects on the hardening
103 of cellular concrete (Fakhratov et al., 2017; Stumm, 2010). These results can serve as a starting point
104 for further studies on the effect of vapo-thermal curing on the hardening of other types of concrete.
105 Hence the idea of combining the production of vegetal concrete with vapo-thermal treatment is **totally**
106 **innovative, and it** can potentially have a significant influence on the improvement of mechanical
107 performances in a perspective of development of green and structural building materials.

108

109 The objective of this study is then to carry out a vapo-thermal treatment on hemp shives in order to
110 understand the influence of this curing on the modification of the hemp structure, from the point of
111 view of their physical, chemical, mineralogical and thermal behaviour. This study is part of an

112 approach of production of a structural vegetal concrete based on hemp shives and lime (lower carbon
 113 footprint than cement). The vapo-thermal treatment is a “green” solution (cure at temperatures below
 114 230°C) that will be used for the hardening of the binder. This experimental investigation is the first
 115 step that provides important informations on the degree of transformation of the hemp under
 116 vapo-thermal curing. Beyond the modified physical properties of the hemp shives following the
 117 different curing conditions, this project is mainly focused on the evolution of the chemical composition
 118 of the plant particles before and after treatment.

119

120 2. Materials and Methods

121 The Raw Hemp Shives (RHS) “Technichanvre” consist of the inner part of the plant dried, defibered
 122 and sifted. These aggregates coming from hemp culture are processed and packaged in France. They
 123 are subject to the "Label Granulat Chanvre", which defines specifications on hemp, and which
 124 ultimately allows the insurability of hemp concrete constructions. The dimensions of the particles are
 125 of the order of 2 to 25 mm. Their color goes from light green to off-white (Fig. 1). Table. 1 presents
 126 the main physical properties of the RHS used.

127



128

129 **Fig. 1** Raw hemp shives

130

131 **Table. 1** Main physical properties of RHS

Physical properties	132
Bulk density (kg/m ³)	110 133
Water retention capacity (ml/l) EN-13041	370 134
pH in suspension at 10%	6.7 – 7.2 135
Thermal conductivity (W/mK)	0.048 136
Specific gravity (Helium pycnometer)	1.5 137

139

140 In our study, hemp shives were dried at 40°C. Four hemp samples of 10g each were placed into tea
 141 balls in a specific autoclave (Fig. 2). The samples underwent a vapo-thermal cure in a closed autoclave
 142 system, under water vapour pressure (5-38 bar) varying according to the temperature based on the
 143 Clausius-Clapeyron equation. Several temperatures were investigated: 150°C, 170°C, 190°C, 210°C

144 and 230°C. The complete cycle **included** 2 hours of temperature rise and four different plateau times
145 (2, 4, 6 and 8 hours). After the vapothermal treatment, the samples **were** dried at 40 °C for 7 days
146 before undergoing the different analyses.

147



148

149 **Fig. 2** Hemp shives in the tea ball, tea ball on the gridded support, tea balls in the autoclave, the
150 autoclave system (From left to right)

151

152 Several parameters **were** monitored before and after vapothermal curing, on dried hemp samples. First
153 of all, visual aspect of hemp samples **was** observed. The color of the shives is an important clue to
154 understand and explain the changes observed on the treated hemp.

155 **Depending on the type of analysis performed, the dried aggregates were finely grinded by a "Retsch**
156 **RS 200" machine.**

157 **Neutral monosaccharide composition (method used by INRA Versailles) was determined on of dried**
158 **alcohol-insoluble material (grinded samples) after hydrolysis in 2.5 M trifluoroacetic acid for 1.5h at**
159 **100°C. To determine the cellulose content, the residual part obtained after the monosaccharide analysis**
160 **was rinsed with water and then hydrolyzed with sulfuric acid H₂SO₄. The released monosaccharides**
161 **were diluted and samples were analysed by HPAEC on an ICS-5000 instrument (Thermo Fisher**
162 **Scientific) with a CarboPac PA20 analytical anion exchange column (3 mm × 150 mm; Thermo Fisher**
163 **Scientific), PA20 guard column (3 mm × 30 mm), borate trap, and a pulsed amperometric detector.**
164 **The samples were eluted using an isocratic gradient of 8 mM NaOH from 0 to 6 min, followed by a**
165 **linear gradient of 8 mM NaOH to 1 mM NaOH from 6 to 23 min. At 23.1 min, the gradient was**
166 **increased to 500 mM NaOH to elute the acidic sugars. Hemicellulose and cellulose contents are**
167 **calculated as weight percentages of the samples.**

168 **For lignin quantification, Klason method based on the insolubility of lignin in a concentrated acid**
169 **medium that hydrolyzes and dissolves the other parietal constituents (cellulose and hemicelluloses) is**
170 **used (Hochegger et al., 2019). 72% of H₂SO₄ is added gradually to samples of alcohol-insoluble**
171 **material in small increments while stirring. The mixture stayed for 2 h in a water bath maintained at 20**
172 **± 1°C while being stirred frequently. Water is added in order to dilute the solution (3% of H₂SO₄). The**
173 **latter is boiled for 4 h maintaining constant volume. The insoluble residue (lignin) is allowed to settle**
174 **until the supernatant solution is clear. The lignin is then transferred quantitatively to the filter using**
175 **hot water. The lignin is washed free of acid with hot water and dried to constant weight in an oven at**

176 105 ± 3°C. The lignin content is calculated from the oven-dry weight of the residue and reported as
177 weight percentage of the sample.

178 The percentage of other proteins and minerals was calculated by subtracting the sum of the
179 percentages of the constituents (hemicellulose, cellulose and lignin) from the total percentage 100%.

180 The thermogravimetric analysis was applied by the thermal analyzer NETZSCH STA 449 F3 Jupiter.
181 The temperature program used ranged from 105 °C to 1000 °C with a ramp of 10 °C/ min.

182 XRD analyses were performed by a BRUKER D8 advance diffractometer, with an angular range of
183 $2\theta=10^\circ-50^\circ$ and a Cobalt anode X-ray tube source (Co-K α : $\lambda = 1,74\text{\AA}$).

184 Loss of mass was determined by mass weighing of the samples (non-grinded) before and after the
185 treatment. Each weighing at a given temperature and time was carried out on four hemp samples of
186 10g each. Water absorption was carried out after drying the aggregates and then calculating their
187 absorption coefficient at 48 hours according to the technical recommendations of RILEM TC 236-
188 BBM (Amziane et al., 2017). Specific gravity (grinded samples) was measured using the Helium
189 pycnometer "micromeritics AccuPyc 1330".

190









191 3. Results and discussion

192 3.1. Visual aspect of hems shives after vapothermal treatment

193 The visual aspect of the hemp shives after vapothermal treatments are presented in **Table. 2**. The
194 treated hemp started to go to a light brown color at the lowest vapothermal temperature (150°C), and
195 ended up with a dark brown color at the temperature of 230°C. At the intermediate temperatures, the
196 treated hemp passes through different shades of brown: slightly dark, dark and very dark. However, no
197 visual difference was noted when curing times are increased from 2 to 8 hours for a fixed temperature.
198 It is also noted that at temperatures above 190°C, the hemp becomes crumbly and loses progressively
199 its integrity.

200

201 **Table. 2** Visual aspect of THS at different temperatures as a function of time

T (°C)	Time (h)			
	2	4	6	8
150				
170				



202

203 The change in color of THS as a function of temperature can therefore be explained by a series of
 204 chemical transformations that the material has undergone between 180 and 250°C, the range
 205 commonly used for the heat treatment of biomass (Esteves and Pereira, 2008). The increase in
 206 temperature and pressure in the autoclave has an effect on the structure of the hemp and modifies its
 207 chemical composition by degrading the cell wall compounds and extractives (Esteves and Pereira,
 208 2008; Sauvageon, 2017). The chemical modifications due to high temperatures depend on the duration
 209 and temperature of the cure, temperature being the main factor.

210 More specifically, the darkening of hemp shives after curing is often explained as the result of the
 211 formation of oxidation and degradation products or low molecular weight sugars that can absorb
 212 visible light. Darkening can also be the result of lignin condensation reactions and the formation of by-
 213 products that contribute to the increase in the intensity of the red tone (Výbohová et al., 2018).

214 The crumbly state observed above 190°C is explained by the fact that the hemp passes gradually by a
 215 progressive carbonization that alters the hemp shives structure.

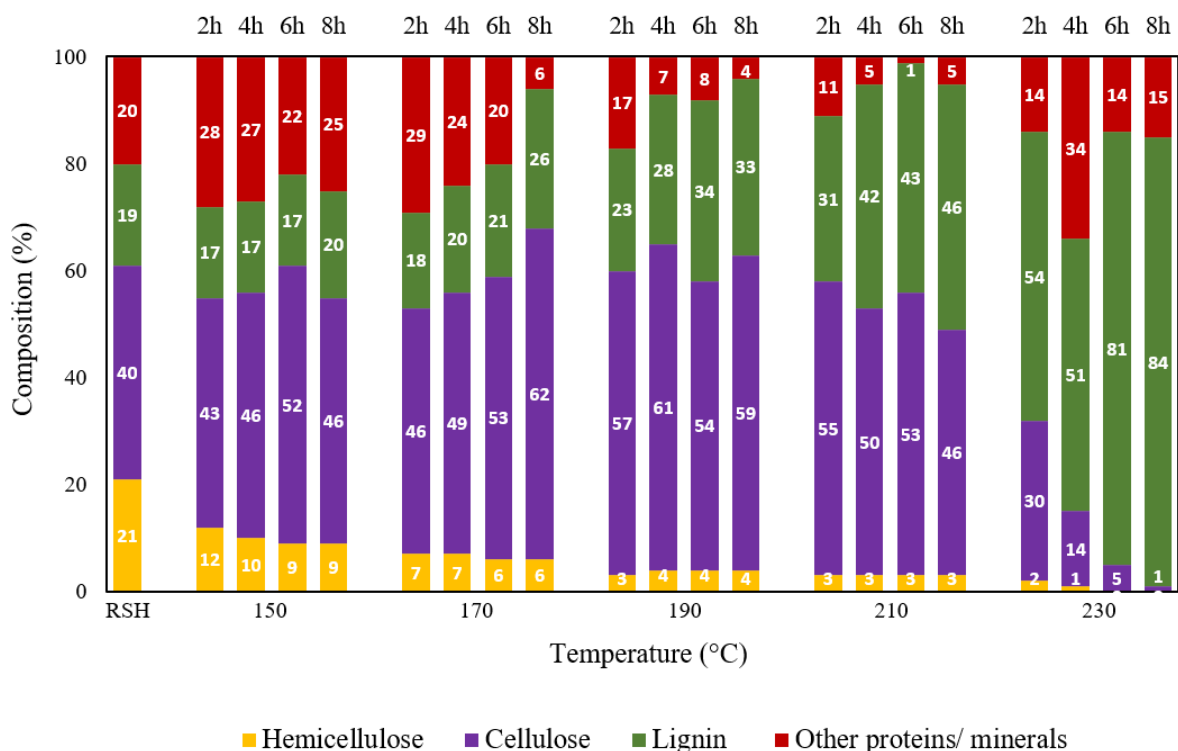
216

217 **3.2. Chemical, thermal and mineralogical modifications of hems shives by vapothermal** 218 **treatment**

219 3.2.1. Chemical composition

220 **Fig. 3** shows the chemical composition of RHS and vapothermal THS. The composition of RHS
 221 shows 21% of hemicellulose, 40% of cellulose, 19% of lignin and 20% of other protein/minerals. The
 222 hemp is mainly composed of cellulose. For the rest of the constituents: hemicellulose, lignin and other
 223 minerals, they are at almost equal amounts. **These results are in agreement with the composition of**
 224 **hemp shives presented in the literature. The percentages of cellulose vary between 12 to 37% for**
 225 **hemicellulose, 34 to 60% for cellulose, 15 to 30% for lignin and 4 to 20% for remainder compounds**

226 (other proteins/minerals) (Belinda, 2005; Delannoy, 2019; Evrard and Erde, 2015; Jami et al., 2019;
 227 Vignon and Dupeyre, 1995).
 228



229
 230 **Fig. 3** Chemical composition (%) of RHS and THS at different temperatures as a function of time
 231
 232 The results show that the vapothermal treatment caused a decrease in the hemicellulose percentage
 233 from 21 % for RHS, to 12% for THS at 150°C for 2 hours. This percentage continued to decrease by
 234 increasing the temperature of the vapothermal treatment until it reaches a value of 0.4% for an 8 hours
 235 cure at 230°C. This can be explained by the fact that hemicelluloses are the first structural compounds
 236 to be thermally affected because of their amorphous nature, even at low temperatures (Kocaeffe et al.,
 237 2008; Rousset et al., 2009; Tumuluru et al., 2011; Yildiz et al., 2006). Degradation begins with
 238 deacetylation of hemicellulose and depolymerization by random cleavage of the glyosidic bonds. The
 239 released acetic acid acts as a catalyst that promotes the decomposition of polysaccharides (Esteves and
 240 Pereira, 2008). Acid-catalyzed degradation leads to the formation of formaldehyde, furfural and other
 241 aldehydes. Furfural and hydroxymethylfurfural are degradation products of pentoses and hexoses,
 242 respectively. At the same time, hemicelluloses undergo dehydration reactions with decreasing
 243 hydroxyl groups (Esteves and Pereira, 2008). The results are compared with observations after
 244 hydrothermal curing because the lack of information for vapothermal treatment.
 245
 246 For cellulose, vapothermal curing caused an increase in the content from 40% for RHS to 43% for a 2
 247 hours treatment at 150°C. This percentage continued to increase to reach values around 50% for cures
 248 up to 210°C. At 230°C, the amount of cellulose dropped to an average of 1% for an 8 hours treatment.

249 Due to the crystalline nature of cellulose, this latter is difficult to degrade (Maniscalco et al., 2020) and
250 starts its decomposition above 210°C. In other studies (Olszewski et al., 2020; Volpe et al., 2020), a
251 complete decomposition of the cellulose was reported at 260°C (Maniscalco et al., 2020). Cellulose
252 can be broken down into water-soluble, lower molecular weight compounds (oligomers) and then into
253 glucose (monomers), which is partially isomerized to fructose. The products of decomposition then
254 undergo a series of isomerization, dehydration and fragmentation (ring opening and C-C bond
255 cleavage), producing intermediates products, 5-HMF or furfural, and their derivatives. These
256 intermediates undergo further polymerization and condensation reactions that lead to the formation of
257 hydrochar (Wang et al., 2018).

258
259 The Klason lignin content decreased from 19% to 17% after a vapothermal cure at 150°C for 2 hours.
260 After this slight decrease, this percentage increased to 84% (230°C for 8 hours). This behavior was
261 observed in some studies where they also found that the lignin content decreases slightly at
262 temperature of 160°C, while it increases at higher temperatures (Výbohová et al., 2018). According to
263 the literature, significant lignin reactions are observed at temperatures above 205°C. These are
264 depolymerization and condensation reactions (Sivonen et al., 2002). Lignin is depolymerized mainly
265 by cleavage of the ether bonds. The cleavage of these bonds is accompanied by an increase in phenolic
266 hydroxyl groups and carbonyl groups (Nuopponen et al., 2004), which are responsible for cross-
267 linking via the formation of methylene bridges (Tjeerdsma et al., 1998; Tjeerdsma and Militz, 2005)
268 and a decrease in aliphatic hydroxyl groups (Tjeerdsma and Militz, 2005). The methoxyl content
269 decreases and new reactive sites on the aromatic ring can lead to further condensation reactions
270 (Wikberg and Maunu, 2004). **At low vapothermal temperatures (150-170°C), decreasing percentages**
271 **are explained by depolymerization and degradation reactions. However, with increasing process**
272 **severity, the rate of carbohydrate degradation (hemicellulose, cellulose) had probably surpassed that of**
273 **decomposition of lignin, resulting in high mass loss values and explains the increased content of**
274 **Klason lignin as seen in other works (Assor et al., 2009; El Hage, 2010; Hochegger et al., 2019;**
275 **Windeisen et al., 2007). The possibility that the lignin content is overestimated by the Klason method**
276 **if such treatment induces some recondensation reactions between polysaccharides (or between**
277 **polysaccharide degradation products) and lignins cannot be excluded (Rousset et al., 2009).**

278
279 As for the rest of the proteins (calculated as the remainder percentage after subtracting the sum of the
280 percentages of cellulose, hemicellulose and lignin), an increase of the percentage from 20% for RSH
281 to 28% for a cure of 2 hours at 150°C. Then, a progressive decrease is observed with the increase of
282 the cure temperature to almost 5% at 210°C (8 hours) explained by the polysaccharides degradation.
283 After this, an increase to 15% is noted at 230°C (8 hours). Most extractives degrade during heat
284 treatment, especially the most volatile ones (Esteves and Pereira, 2008; Maniscalco et al., 2020;
285 Sharma et al., 2020; Yeoh et al., 2018). However, new compounds resulting from the degradation of

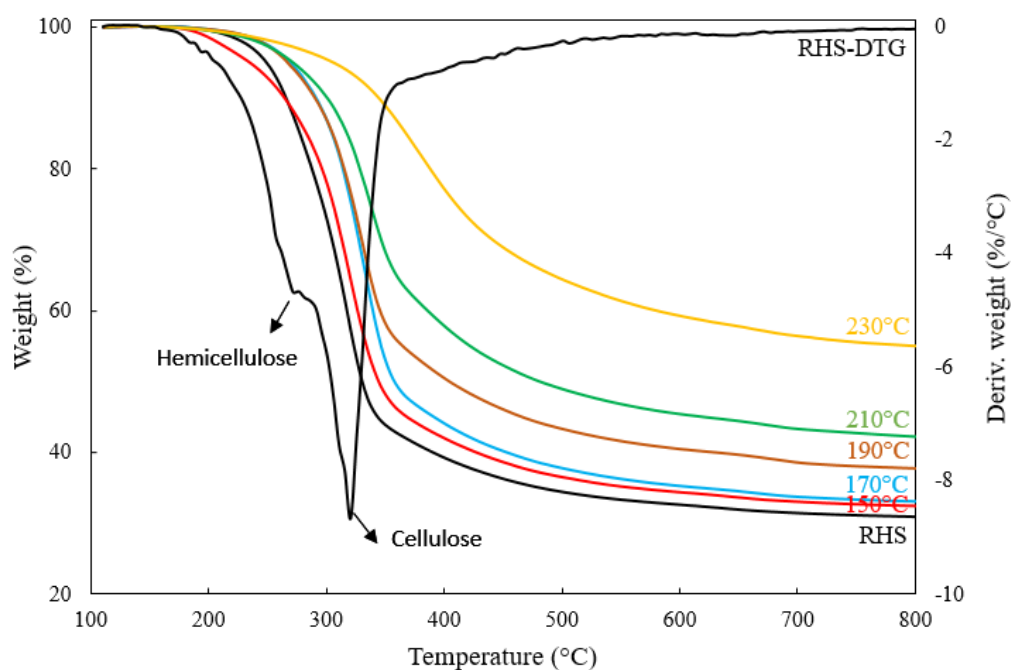
286 structural components of the cell wall can also be formed in the form of extracted waxes,
 287 carbohydrates, tannins and resins (Esteves and Pereira, 2008). The evolution of the proteins/minerals
 288 depends on the balance between the phenomenon of degradation of polysaccharides and the
 289 phenomenon of condensation of certain products such as lignin. The respective rates of these 2
 290 phenomena play a role on the protein and mineral content. **The eventual overestimation of lignin**
 291 **explained in the previous section, may cause an underestimation of the remaining proteins/minerals.**

292
 293 The temperature of 150°C seems to change slightly the chemical structure of hemp shives without
 294 denaturing them. The three main constituents (hemicellulose, cellulose and lignin) are preserved at
 295 percentages similar to those found for RHS.

296
 297 3.2.2. Thermal decomposition

298 **Fig. 4** shows the thermogravimetry TG and differential thermogravimetry DTG curves of RHS and
 299 TG curves for THS at different temperatures for 6 hours.

300



301
 302 **Fig. 4** DTG (%/°C) curve of RHS and TG (%) curves of RHS and THS at different temperatures for 6
 303 hours

304
 305 In the DTG curves, for RHS, the first decomposition shoulder peak at about 180-300°C corresponds
 306 probably to thermal depolymerisation of hemicelluloses or pectin (mass loss 27.5%) and the maximum
 307 mass loss rate is observed at 270°C. In the literature, the first component that is affected by the
 308 vapothermal curing is hemicellulose (Esteves et al., 2008; Esteves and Pereira, 2008) due to its
 309 hydrophilic, amorphous and crosslinked (H-bonds) nature (Farhat, 2018). The decomposition of

310 hemicelluloses vary in the range 180-320°C (Libra et al., 2011; Ouajai and Shanks, 2005; Padilla et
311 al., 2019; Výbohová et al., 2018; Yang et al., 2007). The major second decomposition peak is at about
312 300-360°C (mass loss 29.8%). The maximum mass loss rate was observed at 330°C. In the literature,
313 cellulose decomposition ranges from 315 to 400°C (Ouajai and Shanks, 2005; Padilla et al., 2019;
314 Sevilla and Fuertes, 2009; Yang et al., 2007). Among the three major components, lignin was the most
315 difficult to decompose. It decomposes slowly, over a wide range of temperature from 100 to 900°C
316 (Yang et al., 2007). Some other studies specify that lignin decomposes gradually in a temperature
317 interval of 250-500°C (Fred Shafizadeh, 1985; Khelfa, 2009). Lignin remains degrading even when
318 cellulose and hemicellulose have been completely degraded (Padilla et al., 2019). The complexity of
319 the lignins and the diversity of their structure come from the association of the three monolignols by
320 different chemical bonds without orderly or repetitive character to form an amorphous and
321 hydrophobic polymer (Xun, 2015).

322 Other components, especially extractives, which include monosaccharides (glucose and fructose) and
323 various aldehydic alcohols, aliphatic acids, oligomeric sugars, and phenolic glycosides, are highly
324 reactive in hydrothermal media (Krylova and Zaitchenko, 2018).

325 It should be noted also that the mass loss curve for hems shives treated at 150°C closely resembles to
326 that of the RHS showing that the shives keep their basic chemical structure despite the vapothermal
327 treatment at 150°C.

328
329 Thermal degradation of lignocellulosic biomass is often described by the sum of the thermal behavior
330 of its constituents (Khelfa, 2009). Since the temperature range for the degradation of the constituents
331 is relatively narrow, a high heating rate causes the different maxima in the derived curve to overlap
332 and the temperatures of the characteristic processes tend to become progressively higher. Furthermore,
333 if the temperatures are sufficiently high, significant degradation rates are then simultaneously achieved
334 by all constituents. In other words, although one constituent can be identified respectively as
335 hemicellulose, cellulose and lignin for each zone, the simultaneous participation of the other
336 constituents cannot be avoided (Khelfa, 2009).

337
338 **Table. 3** presents the mass losses noted at the different temperature ranges 180-300°C, 300-360°C and
339 360-900°C. These results are only indicative due to the overlapping of the different mass loss peaks of
340 the 3 main constituents of hemp shives. However, they can give an indication of the evolution of the
341 degradation of the phases.

342
343 **Table. 3** Loss of mass (%) between different temperature ranges for RSH and THS at different curing
344 temperatures for 6 hours

Mass losses (%)	Decomposition T (°C)		
Vapothermal T (°C)	180-300	300-360	360-900
RHS	28	30	12
150	22	31	14
170	14	27	16
190	14	30	18
210	11	25	23
230	5	9	32

346

347 The results show that for RHS, that has not undergone vapothermal treatment, the mass loss between
 348 180 and 300°C (considered to be due to the decomposition of hemicellulose) is 28%, between 300 and
 349 360°C, is 30% (considered to be responsible for the degradation of cellulose) and between 360 and
 350 900°C, is 12% (considered to be at the origin of the decomposition of lignin).

351 Following the increase of the temperature of the vapothermal treatment from 150 to 230°C, the
 352 percentage of mass loss corresponding to the decomposition of hemicellulose decreases to 5%,
 353 showing once again the degradation of hemicellulose by increasing the temperature of the cure.

354 For cellulose, the percentage of mass loss remains around 30% up to 190°C. From 210°C, the mass
 355 losses decrease to a percentage of 9% showing a significant degradation of the cellulose that appears at
 356 temperatures above 210°C.

357 For lignin, mass loss percentages increase progressively up to a value of 32.4% for a vapothermal
 358 treatment at 230°C. If we consider that the percentage of mass loss between 360 and 900°C is an
 359 indication of the evolution of the presence of lignin or recondensation products of lignin in hemp
 360 shives, these increasing percentages can show that the vapothermal treatment allows the
 361 recondensation of lignin products, a phenomena described in literature (Rousset et al., 2009).

362 Mass losses at 150°C demonstrate that this treatment does not denature completely the treated hemp
 363 shives. Indeed, the observed mass losses are of the same order as those noted for the RHS.

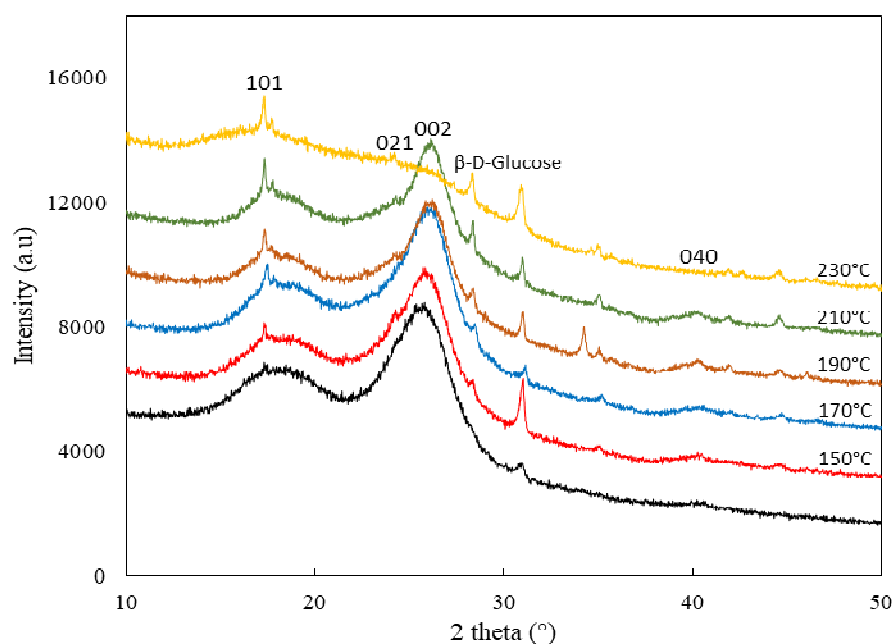
364 All of these results (**Table .3**) are in agreement with the chemical compositions of the different THS
 365 (**Fig .3**), that show that the hemicellulose starts to degrade after the treatment at 150°C, while the
 366 decomposition of the cellulose only takes place at temperatures of 210°C and finally the lignin, the
 367 most difficult component to degrade, does not show signs of degradation at least up to temperatures of
 368 230°C, however the latter can show signs of condensation reactions.

369

370 3.2.3. Mineralogical composition

371 For XRD analysis, as the patterns are similar for the different vapothermal treatment times, only
 372 results of treatments for 6 hours are presented (**Fig. 5**). For temperatures below 210°C, it can be

373 observed that XRD pattern for THS are similar to that of RHS, indicating that the crystalline structure
374 has been preserved. Patterns show the following peaks: $\sim 16^\circ(101)$, $\sim 19^\circ(101)$, $\sim 24^\circ(021)$, $\sim 26^\circ(002)$,
375 and $\sim 40^\circ(040)$. These signatures are characteristic of cellulose I (Dash et al., 2020; Roumeli et al.,
376 2015; Sevilla and Fuertes, 2009; Udoetok et al., 2018). Among the main constituents of hemp shives,
377 cellulose is the only molecule that have a crystalline nature that can be detected by XRD.
378 In addition to the peaks of cellulose, two other peaks around 28° and 31° appear for THS at all cure
379 temperatures. These two peaks are identified as peaks corresponding to the presence of β -D-Glucose.
380



381
382 **Fig. 5** XRD patterns of RHS and THS at different temperatures for 6 hours
383

384 The crystallinity of the cellulose depends on the temperature of the hydrothermal cure (Esteves and
385 Pereira, 2008; Michiel Boonstra, 2008). Up to temperatures of 210°C , the crystallinity increases due to
386 the degradation of the less ordered parts of the cellulose (Michiel Boonstra, 2008). The hydroxyl
387 groups of cellulose degrade in the following order: amorphous, semi-crystalline and crystalline
388 (Wikberg and Maunu, 2004). On the other hand, pattern obtained at temperature of 230°C is no longer
389 crystalline, as can be inferred from the absence of reflections in the X-ray pattern, according with
390 literature (Sevilla and Fuertes, 2009). The crystallinity of cellulose increases due to the degradation of
391 amorphous cellulose, leading to a decrease in the accessibility of hydroxyl groups to water molecules,
392 which contributes to a decrease in the hydrophilic character of the plant aggregates (Esteves and
393 Pereira, 2008).

394
395 As for Glucose peaks, their presence can be explained by the fact that hemicellulose and cellulose
396 degradations (even at the amorphous parts), proceed via cleavage of mainly β -(1-4) glycosidic bonds

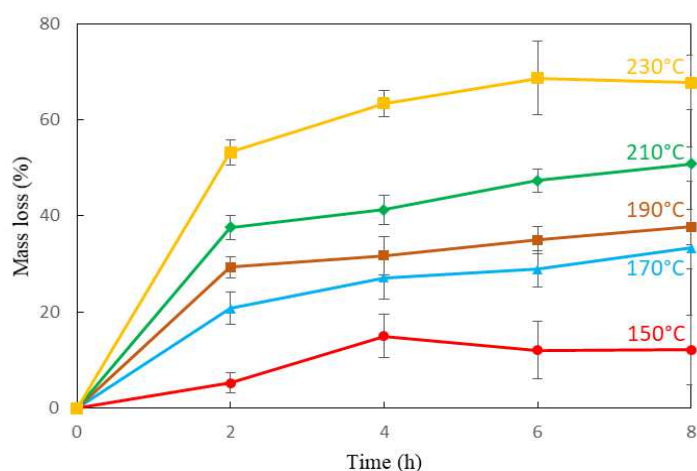
397 and cause the release of glucose monomers (Esteves and Pereira, 2008; Krylova and Zaitchenko,
398 2018).

399

400 **3.3. Physical modification of hems shives by vapothermal treatment**

401 3.3.1. Mass loss

402 **Fig. 6** summarizes the yield results of mass loss calculations (four hemp samples of 10g for each
403 temperature and time curing) at different temperatures in function of time. As mentioned before, at
404 temperatures above 190°C the hemp becomes crumbly and causes a very slight loss of material in the
405 autoclave. As a result, the mass losses noted for temperatures of 210°C and 230°C may be less
406 accurate, but can still be indicative.



407

408 **Fig. 6** Mass losses (%) of THS at different temperatures as a function of time

409

410 At a fixed time of curing, the percentages of mass loss increase with increasing temperature. For
411 example, after 2 hours of curing, the loss of mass passes from 5.2% at T=150°C to 29.3% at T=190°C
412 and reaches 53.3% at 230°C. These percentages increase also with the treatment time duration. The
413 mass loss percentage at 190°C passes from 29.3% at 2 hours to 37.7% after 8 hours of treatment.

414 According to the results obtained, the average loss of mass of the hemp increases as the temperature of
415 the cure increases, which is in accordance with the conclusions of previous studies showing the loss of
416 mass of hydrothermal treated biomass in function of the temperature used (Wang et al., 2018; Zhang
417 et al., 2020). Different types of plants (rapeseed straw, oil palm biomass...) have been treated under
418 hydrothermal curing from 170 to 230°C (Díaz et al., 2010; Zakaria et al., 2015).

419 These mass losses confirm the presence of chemical transformations that occur under the effect of the
420 increase in temperature and pressure and that may include removal of volatiles (Esteves and Pereira,
421 2008; Maniscalco et al., 2020; Sharma et al., 2020; Yeoh et al., 2018). Unlike the visual aspect which
422 does not change according to the duration of the treatment, mass losses increase from 2 to 8 hours of
423 treatment at all temperature curing.

424

425 3.3.2. Water absorption

426 Water absorption for RHS is 335%. **Table. 4** presents the results of the quantities of water absorbed
 427 (%) at 48 hours by the hemp following the different vapothermal treatments.

428

429 **Table. 4** Water content (%) at 48 hours of THS at different temperatures as a function of time

T (°C)	Time (h)			
	2	4	6	8
150	319 ± 1	325 ± 4	314 ± 6	328 ± 2
170	265 ± 4	282 ± 7	269 ± 2	274 ± 4
190	249 ± 5	234 ± 2	218 ± 7	240 ± 5

430

431 Based on these results, it can be seen that the absorption coefficient decreases after vapothermal
 432 treatments. It passes from 335% without treatment, to 314% for a cure at 150°C showing an absorption
 433 decrease of 6.3%. Absorption coefficient continues to decrease in function of temperature until it
 434 reaches 218% at 190°C (a decrease of 34.9%). For this test, absorptions at 210°C and 230°C were not
 435 measured as the hemp shives turned to a carbonized crumbly state.

436 Vapothermal treatment causes a decrease in water absorption due to a chemical change in the structure
 437 of the hemp during the vapothermal cure. In literature, after hydrothermal curing, this fact was
 438 explained by the increased crystallinity of the cellulose due to the degradation or to the crystallization
 439 of amorphous cellulose (or both) (Michiel Boonstra, 2008), causing decreased accessibility of
 440 hydroxyl groups to water molecules (Esteves and Pereira, 2008). The decrease in water absorption can
 441 also be explained by the cross-linking of lignin caused after hydrothermal treatment that may also play
 442 a role in the decrease of the amount of water absorbed by the hemp, which improves the
 443 hydrophobicity of THS (Pejic et al., 2008; Sivonen et al., 2002).

444

445 3.3.3. Specific gravity

446 Specific gravity of RHS is 1.5. **Table. 5** shows the specific gravities of hemp treated under different
 447 conditions. The values for the THS do not differ much from each other (1.43-1.49). The values
 448 obtained show that the vapothermal cure causes a decrease in the specific gravity of the hemp shives.
 449 The results for temperatures above 190°C will not be presented for the same reason cited before.

450

451 **Table. 5** Specific gravities of THS at different temperatures as a function of time

T (°C)	Time (h)			
	2	4	6	8
150	1.49	1.46	1.49	1.43
170	1.44	1.45	1.43	1.42

190	1.49	1.43	1.44	1.44
-----	------	------	------	------

452

453 The decrease in the specific gravity can be explained by the loss of mass (degradation reactions of
 454 different constituents of hemp shives into volatile products) of THS seen after the vapothermal
 455 treatment (**Fig. 6**).

456

457 All these physical changes are the result of modifications and transformations in the composition of
 458 the treated hemp shives.

459

460 **4. Conclusions**

461 The main objective of the work was the evaluation of the effect of vapothermal curing **on the chemical**
 462 **(composition in cellulose, hemicellulose and lignin)** and physical **properties** (mass loss, absorption
 463 coefficient and specific gravity) of hemp shives, **as aggregates that can enter in the production of**
 464 **structural vegetal concrete. The idea of the production of vapothermal treated vegetal concrete is**
 465 **totally innovative, and can make it possible to overcome of the compatibility problem with**
 466 **cementitious matrix (improvement of mechanical performances in a perspective of development of**
 467 **green and structural building materials).**

468 As a result, hemp **shives** underwent different vapothermal cures at temperatures of 150°, 170°, 190°,
 469 210° and 230°C.

470 The main conclusions drawn are:

471 -The color of the hemp shives becomes darker and go through a progressive carbonization, and the
 472 loss of mass increases as the temperature of the vapothermal cure increases.

473 -The water absorption coefficient decreases with the temperature of the cure, but still not enough for a
 474 good compatibility in cement interaction, while the specific gravity decreases after the vapothermal
 475 treatment and remains unchanged with increasing cure temperature.

476 -These physical changes during a vapothermal treatment are associated with chemical transformations
 477 that take place into the structure of the treated hemp, thus changing the chemical composition of the
 478 hemp.

479 These changes can be summarized by:

480 -The depolymerization of hemicellulose, which is the first component that starts to be affected by the
 481 cure at low temperatures (150°C)

482 -The increase in the crystallinity of the cellulose accompanied by a decrease in the hydrophilic sites
 483 and leading to a drop in the absorption coefficient even at low curing temperatures (<210°C). Towards
 484 higher temperatures (>210°C), cellulose no longer resists to degradation.

485 -As for lignin, it depolymerizes at temperatures close to 190°C. However, condensation reactions of
 486 degradation products can occur.

487

488 This study that determined the effect of vapothermal curing on the physicochemical properties of
489 hemp shives, constitutes the first step in the approach of the formulation of autoclaved structural hemp
490 concrete for civil engineering applications. Therefore, a vapothermal treatment at 150°C seems to be
491 the curing process that allows to preserve the chemical structure of the hemp shives.

492

493 **References**

494 Aderinsola Sadiku, N., Sanusi, A., 2014. Wood pre-treatment influence on the hydration of portland
495 cement in combination with some tropical wood species. *Pro Ligno* 10, 3–10.

496 Amziane, S., 2016. Overview on biobased building material made with plant aggregate. *Sustain.*
497 *Constr. Mater. Technol.* 2016-Augus, 31–38. <https://doi.org/10.21809/rilemtechlett.v1.9>

498 Amziane, S., Arnaud, L., 2013. Bio-aggregate-based Building Materials: Applications to Hemp
499 Concretes, Wiley-ISTE. ed.

500 Amziane, S., Collet, F., Lawrence, M., Magniont, C., Picandet, V., Sonebi, M., 2017.
501 Recommendation of the RILEM TC 236-BBM: characterisation testing of hemp shiv to
502 determine the initial water content, water absorption, dry density, particle size distribution and
503 thermal conductivity. *Mater. Struct. Constr.* 50. <https://doi.org/10.1617/s11527-017-1029-3>

504 Assor, C., Placet, V., Chabbert, B., Habrant, A., Lapierre, C., Pollet, B., Perré, P., 2009. Concomitant
505 Changes in Viscoelastic Properties and Amorphous Polymers during the Hydrothermal
506 Treatment of Hardwood and Softwood. *J. Agric. Food Chem.* 57, 6830–6837.
507 <https://doi.org/10.1021/jf901373s>

508 Belinda, A., 2005. chemical composition of the fibres Hemp raw materials : The effect of cultivar ,
509 growth conditions and pretreatment on the chemical composition of the fibres.

510 Biller, P., Ross, A.B., 2016. Production of biofuels via hydrothermal conversion, *Handbook of*
511 *Biofuels Production: Processes and Technologies: Second Edition.* Elsevier Ltd.
512 <https://doi.org/10.1016/B978-0-08-100455-5.00017-5>

513 Commissariat Général au Développement Durable, 2020. Data Lab: Chiffres clés du climat - France,
514 Europe et Monde - Édition 2020.

515 Dash, C., Das, A., Kumar Bisoyi, D., 2020. Influence of pretreatment on mechanical and dielectric
516 properties of short sunn hemp fiber-reinforced polymer composite in correlation with fine
517 structure of the fiber. *J. Compos. Mater.* 54, 3313–3327.
518 <https://doi.org/10.1177/0021998320914071>

519 Delannoy, G., 2019. Durabilité d'isolants à base de granulats végétaux. Thèse de doctorat de
520 l'Université Paris-Est.

521 Díaz, M.J., Cara, C., Ruiz, E., Romero, I., Moya, M., Castro, E., 2010. Hydrothermal pre-treatment of
522 rapeseed straw. *Bioresour. Technol.* 101, 2428–2435.
523 <https://doi.org/10.1016/j.biortech.2009.10.085>

524 El Hage, R., 2010. Prétraitement du *Miscanthus x giganteus* . Vers une valorisation optimale de la

525 biomasse. Thèse de doctorat de l'Université de Nancy.

526 Esteves, B.M., Domingos, I.J., Pereira, H.M., 2008. Pine wood modification by heat treatment in air.
527 *BioResources* 3, 142–154. <https://doi.org/10.15376/biores.3.1.142-154>

528 Esteves, B.M., Pereira, H.M., 2008. Wood modification by heat treatment: A review. *BioResources* 4,
529 370–404. <https://doi.org/10.15376/biores.4.1.370-404>

530 Evrard, A., Erde, L.T., 2015. Transient hygrothermal behavior of Lime-Hemp Materials Ecole
531 Polytechnique de Louvain Unité d'Architecture Transient hygrothermal behaviour of Lime-
532 Hemp Materials Thèse présentée en vue de l'obtention du doctorat en Sciences de l'Ingénieur
533 par Comit.

534 Fakhratov, M., Erkenov, R., Kulchaev, A., Zavgorodniy, A., 2017. Manufacturing processes of
535 cellular concrete products for the construction, in: *MATEC Web of Conferences*.
536 <https://doi.org/10.1051/mateconf/201711700043>

537 Farhat, W., 2018. Investigation of Hemicellulose Biomaterial Approaches: The Extraction and
538 Modification of Hemicellulose and its Use in Value-added Applications. Thèse de doctorat de
539 l'Université de Lyon.

540 Fontana, P., Lehmann, C., Muller, U., 2009. Influence of hydrothermal curing on micro structure and
541 mechanical properties of ultra-high performance concrete. *Brittle Matrix Compos.* 9, BMC 2009
542 391–398. <https://doi.org/10.1533/9781845697754.391>

543 Fred Shafizadeh, 1985. *Fundamentals of thermochemical biomass conversion*. Elsevier Ltd, London
544 and New York.

545 Funke, A., Reeb, F., Kruse, A., 2013. Experimental comparison of hydrothermal and vapothermal
546 carbonization. *Fuel Process. Technol.* 115, 261–269.
547 <https://doi.org/10.1016/j.fuproc.2013.04.020>

548 Galvánková, L., Másilko, J., Solný, T., Štěpánková, E., 2016. Tobermorite Synthesis under
549 Hydrothermal Conditions. *Procedia Eng.* 151, 100–107.
550 <https://doi.org/10.1016/j.proeng.2016.07.394>

551 Gartner, E., 2004. Industrially interesting approaches to “low-CO₂” cements. *Cem. Concr. Res.* 34,
552 1489–1498. <https://doi.org/10.1016/j.cemconres.2004.01.021>

553 German Patent Nr. DE 10 2009 010 233 A1, 2009, 2009. Verfahren zur Gewinnung von Rohstoff und
554 Energieträgern aus Pflanzen und Pflanzenreste.

555 Guillot, M., 2019. Etude du traitement de la biomasse par voie hydrothermale pour la récupération de
556 molécules et de minéraux à haute valeur ajoutée. Thèse de doctorat de l'Université Montpellier
557 II.

558 Hillis, W.E., 1984. High temperature and chemical effects on wood stability. *Wood Sci. Technol.* 18,
559 281–293. <https://doi.org/10.1007/bf00353364>

560 Hohegger, M., Cottyn-Boitte, B., Cézard, L., Schober, S., Mittelbach, M., 2019. Influence of Ethanol
561 Organosolv Pulping Conditions on Physicochemical Lignin Properties of European Larch. *Int. J.*

562 Chem. Eng. 2019, 1–10. <https://doi.org/10.1155/2019/1734507>

563 Huang, H.J., Yuan, X.Z., 2016. The migration and transformation behaviors of heavy metals during
564 the hydrothermal treatment of sewage sludge. *Bioresour. Technol.* 200, 991–998.
565 <https://doi.org/10.1016/j.biortech.2015.10.099>

566 Jami, T., Karade, S.R., Singh, L.P., 2019. A review of the properties of hemp concrete for green
567 building applications. *J. Clean. Prod.* 239, 117852. <https://doi.org/10.1016/j.jclepro.2019.117852>

568 Khazma, M., Goullieux, A., Dheilily, R.M., Laidoudi, B., Queneudec, M., 2011. Impact of aggregate
569 coating with a PEC elastomer on properties of lightweight flax shive concrete. *Ind. Crops Prod.*
570 33, 49–56. <https://doi.org/10.1016/j.indcrop.2010.08.005>

571 Khazma, M., Goullieux, A., Dheilily, R.M., Quéneudec, M., 2012. Coating of a lignocellulosic
572 aggregate with pectin/polyethylenimin mixtures: Effects on flax shive and cement-shive
573 composite properties. *Cem. Concr. Compos.* 34, 223–230.
574 <https://doi.org/10.1016/j.cemconcomp.2011.07.008>

575 Khazma, M., Goullieux, A., Dheilily, R.M., Rougier, A., Quéneudec, M., 2014. Optimization of flax
576 shive-cementitious composites: Impact of different aggregate treatments using linseed oil. *Ind.*
577 *Crops Prod.* 61, 442–452. <https://doi.org/10.1016/j.indcrop.2014.07.041>

578 Khelfa, A., 2009. Etude des étapes primaires de la dégradation thermique de la biomasse
579 lignocellulosique. Thèse de doctorat de l'Université Paul Verlaine.

580 Kocafe, D., Poncsak, S., Boluk, Y., 2008. Effect of thermal treatment on the chemical composition
581 and mechanical properties of birch and aspen. *BioResources* 3, 517–537.
582 <https://doi.org/10.15376/biores.3.2.517-537>

583 Krylova, A.Y., Zaitchenko, V.M., 2018. Hydrothermal Carbonization of Biomass: A Review. *Solid*
584 *Fuel Chem.* 52, 91–103. <https://doi.org/10.3103/S0361521918020076>

585 Libra, J.A., Ro, K.S., Kammann, C., Funke, A., Berge, N.D., Neubauer, Y., Titirici, M.M., Fühner, C.,
586 Bens, O., Kern, J., Emmerich, K.H., 2011. Hydrothermal carbonization of biomass residuals: A
587 comparative review of the chemistry, processes and applications of wet and dry pyrolysis.
588 *Biofuels* 2, 71–106. <https://doi.org/10.4155/bfs.10.81>

589 Maniscalco, M.P., Volpe, M., Messineo, A., 2020. Hydrothermal Carbonization as a Valuable Tool for
590 Energy and Environmental Applications: A Review. *Energies* 13, 4098.
591 <https://doi.org/10.3390/en13164098>

592 Michiel Boonstra, 2008. A two-stage thermal modification of wood. Thèse de doctorat de l'Université
593 Henri Poincaré.

594 Miranda de Lima, A.J., Iwakiri, S., Lomeli-Ramírez, M.G., 2015. Study of the Interaction of Portland
595 Cement and Pinus Wood for Composites using Bragg Sensors in Optical Fibers. *BioResources*
596 10. <https://doi.org/10.15376/biores.10.4.6690-6704>

597 Nozahic, V., 2012. Vers une nouvelle démarche de conception des bétons de végétaux
598 lignocellulosiques basée sur la compréhension et l'amélioration de l'interface liant / végétal :

599 application à des granulats de chenevotte et de tige de tournesol associés à un liant ponce /
600 Thèse de doctorat de l'Université Blaise Pascal - Clermont-Ferrand II.

601 Nuopponen, M., Vuorinen, T., Jämsä, S., Viitaniemi, P., 2004. Thermal modifications in softwood
602 studied by FT-IR and UV resonance Raman spectroscopies. *J. Wood Chem. Technol.* 24, 13–26.
603 <https://doi.org/10.1081/WCT-120035941>

604 Olszewski, M.P., Nicolae, S.A., Arauzo, P.J., Titirici, M.M., Kruse, A., 2020. Wet and dry? Influence
605 of hydrothermal carbonization on the pyrolysis of spent grains. *J. Clean. Prod.* 260, 121101.
606 <https://doi.org/10.1016/j.jclepro.2020.121101>

607 Ouajai, S., Shanks, R.A., 2005. Composition, structure and thermal degradation of hemp cellulose
608 after chemical treatments. *Polym. Degrad. Stab.* 89, 327–335.
609 <https://doi.org/10.1016/j.polyimdegradstab.2005.01.016>

610 Padilla, E.R.D., Nakashima, G.T., Hansted, A.L.S., Santos, L.R.O., De Barros, J.L., De Conti, A.C.,
611 Yamaji, F.M., 2019. Thermogravimetric and FTIR analyzes of corn cob pyrolysis. *Quim. Nova*
612 42, 566–569. <https://doi.org/10.21577/0100-4042.20170360>

613 Pasca, S.A., Hartley, I.D., Reid, M.E., Thring, R.W., 2010. Evaluation of Compatibility between
614 Beetle-Killed Lodgepole Pine (*Pinus Contorta* var. *Latifolia*) Wood with Portland Cement.
615 *Materials (Basel)*. 3, 5311–5319. <https://doi.org/10.3390/ma3125311>

616 Pejic, B.M., Kostic, M.M., Skundric, P.D., Praskalo, J.Z., 2008. The effects of hemicelluloses and
617 lignin removal on water uptake behavior of hemp fibers. *Bioresour. Technol.* 99, 7152–7159.
618 <https://doi.org/10.1016/j.biortech.2007.12.073>

619 Peterson, A.A., Vogel, F., Lachance, R.P., Fröling, M., Antal, M.J., Tester, J.W., 2008.
620 Thermochemical biofuel production in hydrothermal media: A review of sub- and supercritical
621 water technologies. *Energy Environ. Sci.* 1, 32–65. <https://doi.org/10.1039/b810100k>

622 Roumeli, E., Terzopoulou, Z., Pavlidou, E., Chrissafis, K., Papadopoulou, E., Athanasiadou, E.,
623 Triantafyllidis, K., Bikiaris, D.N., 2015. Effect of maleic anhydride on the mechanical and
624 thermal properties of hemp/high-density polyethylene green composites. *J. Therm. Anal.*
625 *Calorim.* 121, 93–105. <https://doi.org/10.1007/s10973-015-4596-y>

626 Rousset, P., Lapierre, C., Pollet, B., Quirino, W., Perre, P., 2009. Effect of severe thermal treatment on
627 spruce and beech wood lignins. *Ann. For. Sci.* 66, 110–110.
628 <https://doi.org/10.1051/forest/2008078>

629 Rulkens, W., 2008. Sewage Sludge as a Biomass Resource for the Production of Energy: Overview
630 and Assessment of the Various Options. *Energy & Fuels* 22, 9–15.
631 <https://doi.org/10.1021/ef700267m>

632 Sauvageon, T., 2017. Caractérisation et valorisation de fibres de chanvre issues de sols et de matériels
633 délaissés : cas du traitement par explosion à la vapeur. Thèse de doctorat de l'Université de
634 Lorraine.

635 Sevilla, M., Fuertes, A.B., 2009. The production of carbon materials by hydrothermal carbonization of

636 cellulose. *Carbon* N. Y. 47, 2281–2289. <https://doi.org/10.1016/j.carbon.2009.04.026>

637 Shafie, S.A., Al-attab, K.A., Zainal, Z.A., 2018. Effect of hydrothermal and vapothermal
638 carbonization of wet biomass waste on bound moisture removal and combustion characteristics.
639 *Appl. Therm. Eng.* 139, 187–195. <https://doi.org/10.1016/j.applthermaleng.2018.02.073>

640 Sharma, R., Jasrotia, K., Singh, N., Ghosh, P., srivastava, S., Sharma, N.R., Singh, J., Kanwar, R.,
641 Kumar, A., 2020. A Comprehensive Review on Hydrothermal Carbonization of Biomass and its
642 Applications. *Chem. Africa* 3, 1–19. <https://doi.org/10.1007/s42250-019-00098-3>

643 Sivonen, H., Maunu, S.L., Sundholm, F., Jämsä, S., Viitaniemi, P., 2002. Magnetic resonance studies
644 of thermally modified wood. *Holzforschung* 56, 648–654. <https://doi.org/10.1515/HF.2002.098>

645 Stumm, A., 2010. Method for the production of cellular concrete and foamed concrete, and system for
646 carrying out the method. US 2010/0252946 A1.

647 Titirici, M.M., Funke, A., Kruse, A., 2015. Hydrothermal Carbonization of Biomass. *Recent Adv.*
648 *Thermochem. Convers. Biomass* 325–352. <https://doi.org/10.1016/B978-0-444-63289-0.00012-0>

649 Tjeerdsma, B.F., Boonstra, M., Pizzi, A., Tekely, P., Militz, H., 1998. Characterisation of thermally
650 modified wood: Molecular reasons for wood performance improvement. *Holz als Roh - und*
651 *Werkst.* 56, 149–153. <https://doi.org/10.1007/s001070050287>

652 Tjeerdsma, B.F., Militz, H., 2005. Chemical changes in hydrothermal treated wood: FTIR analysis of
653 combined hydrothermal and dry heat-treated wood. *Holz als Roh - und Werkst.* 63, 102–111.
654 <https://doi.org/10.1007/s00107-004-0532-8>

655 Toor, S.S., Rosendahl, L., Rudolf, A., 2011. Hydrothermal liquefaction of biomass: A review of
656 subcritical water technologies. *Energy* 36, 2328–2342.
657 <https://doi.org/10.1016/j.energy.2011.03.013>

658 Tumuluru, J.S., Sokhansanj, S., Hess, J.R., Wright, C.T., Boardman, R.D., 2011. A review on biomass
659 torrefaction process and product properties for energy applications. *Ind. Biotechnol.* 7, 384–401.
660 <https://doi.org/10.1089/ind.2011.7.384>

661 Udoetok, I.A., Wilson, L.D., Headley, J. V., 2018. "Pillaring Effects " in *Cross-Linked Cellulose*
662 *Biopolymers: A Study of Structure and Properties.* *Int. J. Polym. Sci.* 2018.
663 <https://doi.org/10.1155/2018/6358254>

664 United Nations Environment Programme, 2009. Annual report seizing the green opportunity.

665 Vignon, M.R., Dupeyre, D., 1995. Steam explosion of woody hemp chènevotte. *Int. J. Biol.*
666 *Macromol.* 17, 395–404.

667 Vogel, F., 2019. Hydrothermal Conversion of Biomass, in: *Energy from Organic Materials (Biomass).*
668 Springer, New York, pp. 1251–1295. https://doi.org/10.1007/978-1-4939-7813-7_993

669 Volpe, M., Messineo, A., Mäkelä, M., Barr, M.R., Volpe, R., Corrado, C., Fiori, L., 2020. Reactivity
670 of cellulose during hydrothermal carbonization of lignocellulosic biomass. *Fuel Process.*
671 *Technol.* 206, 106456. <https://doi.org/10.1016/j.fuproc.2020.106456>

672 Výbohová, E., Kučerová, V., Andor, T., Balážová, Ž., Veřková, V., 2018. The Effect of Heat

673 Treatment on the Chemical Composition of Ash Wood. *BioResources* 13.
674 <https://doi.org/10.15376/biores.13.4.8394-8408>

675 Wang, T., Zhai, Y., Zhu, Y., Li, C., Zeng, G., 2018. A review of the hydrothermal carbonization of
676 biomass waste for hydrochar formation: Process conditions, fundamentals, and physicochemical
677 properties. *Renew. Sustain. Energy Rev.* 90, 223–247. <https://doi.org/10.1016/j.rser.2018.03.071>

678 Wikberg, H., Maunu, S.L., 2004. Characterisation of thermally modified hard- And softwoods by ¹³C
679 CPMAS NMR. *Carbohydr. Polym.* 58, 461–466. <https://doi.org/10.1016/j.carbpol.2004.08.008>

680 Windeisen, E., Strobel, C., Wegener, G., 2007. Chemical changes during the production of thermo-
681 treated beech wood. *Wood Sci. Technol.* 41, 523–536. [https://doi.org/10.1007/s00226-007-0146-](https://doi.org/10.1007/s00226-007-0146-5)
682 5

683 Xun, L., 2015. Valorisation énergétique de la biomasse lignocellulosique par digestion anaérobie :
684 prétraitement fongique aérobie. Thèse de doctorat de l'INSA Lyon.

685 Yang, H., Yan, R., Chen, H., Lee, D.H., Zheng, C., 2007. Characteristics of hemicellulose, cellulose
686 and lignin pyrolysis. *Fuel* 86, 1781–1788. <https://doi.org/10.1016/j.fuel.2006.12.013>

687 Yeoh, K.H., Shafie, S.A., Al-attab, K.A., Zainal, Z.A., 2018. Upgrading agricultural wastes using
688 three different carbonization methods: Thermal, hydrothermal and vapothermal. *Bioresour.*
689 *Technol.* 265, 365–371. <https://doi.org/10.1016/j.biortech.2018.06.024>

690 Yildiz, S., Gezer, E.D., Yildiz, U.C., 2006. Mechanical and chemical behavior of spruce wood
691 modified by heat. *Build. Environ.* 41, 1762–1766. <https://doi.org/10.1016/j.buildenv.2005.07.017>

692 Zakaria, M.R., Hirata, S., Hassan, M.A., 2015. Hydrothermal pretreatment enhanced enzymatic
693 hydrolysis and glucose production from oil palm biomass. *Bioresour. Technol.* 176, 142–148.
694 <https://doi.org/10.1016/j.biortech.2014.11.027>

695 Zhang, L., Lyu, S., Zhang, Q., Chmely, S.C., Wu, Y., Melcher, C., Rajan, K., Harper, D.P., Wang, S.,
696 Chen, Z., 2020. Recycling hot-water extractions of lignocellulosic biomass in bio-refinery for
697 synthesis of carbon nanoparticles with amplified luminescence and its application in temperature
698 sensing. *Ind. Crops Prod.* 145. <https://doi.org/10.1016/j.indcrop.2019.112066>
699